Data-independent acquisition parallel accumulation-serial fragmentation (diaPASEF) analysis of the separated zebrafish lens improves identifications

Sarah R. Zelle[1], W. Hayes McDonald[2], Kristie L. Rose[2], Hassane S. Mchaourab[3], Kevin L. Schey[2]

[1]Chemical and Physical Biology Program, Vanderbilt University, Nashville, Tennessee

[2]Department of Biochemistry, Vanderbilt University, Nashville, Tennessee

[3]Department of Molecular Physiology and Biophysics, Vanderbilt University, Nashville, Tennessee

Corresponding Author:
Kevin L. Schey
465 21st Ave South
MRB III, Bio/Sci 9160
Nashville, TN 37232
Email: k.schey@vanderbilt.edu

Conflicts of Interest: None

Keywords: DIA, diaPASEF, proteomics, zebrafish, lens, aging

Abstract

Ocular lens fiber cells degrade their organelles during differentiation to prevent light scattering. Organelle degradation occurs continuously throughout an individual's lifespan, creating a spatial gradient of young cortical fiber cells in the lens periphery to older nuclear fiber cells in the center of the lens. Therefore, separation of cortical and nuclear regions enables examination of protein aging. Previously, the human lens cortex and nucleus have been studied using data-independent acquisition (DIA) proteomics, allowing for the identification of low-abundance protein groups. In this study, we employed data-independent acquisition parallel accumulation-serial fragmentation (diaPASEF) proteomics on a timsTOF HT instrument to study the zebrafish lens proteome and compared results to a standard DIA method employed on an Orbitrap Exploris 480. Using the additional ion mobility gas phase separation of diaPASEF, peptide and protein group identifications increased by over 200% relative to an orbitrap DIA method in the zebrafish lens. With diaPASEF, we identified 13,721 and 11,996 unique peptides in the zebrafish lens cortex and nucleus, respectively, which correspond to 1,537 and 1,389 protein groups. Thus, separation of the zebrafish lens into cortical and nuclear regions followed by diaPASEF analysis produced the most comprehensive zebrafish lens proteomic dataset to date.

Introduction

The lens is a transparent organ that focuses light onto the retina. With age, the lens becomes opacified and scatters light, a condition known as cataract, the leading cause of blindness worldwide.[1–3] Cellular organelles act as potential sources of light scattering, so during lens fiber cell differentiation, organelles are degraded.[1] As we age, continual lens fiber cell differentiation creates a spatial gradient of young cortical fiber cells to old nuclear fiber cells (Figure 1).[2–4] Due to the loss of organelles during differentiation, there is no protein turnover in nuclear lens fiber cells, and proteins synthesized at birth remain in the nucleus for the lifespan of an individual.[5] Lens fiber cell differentiation thus creates a continuum of regions with distinct proteomes in the lens, necessitating the separation of lens regions to examine age-related proteome changes. Conventionally, the lens is separated into organelle-containing cortical and organelle-free nuclear regions for spatiotemporal proteomic analyses.[5,6]

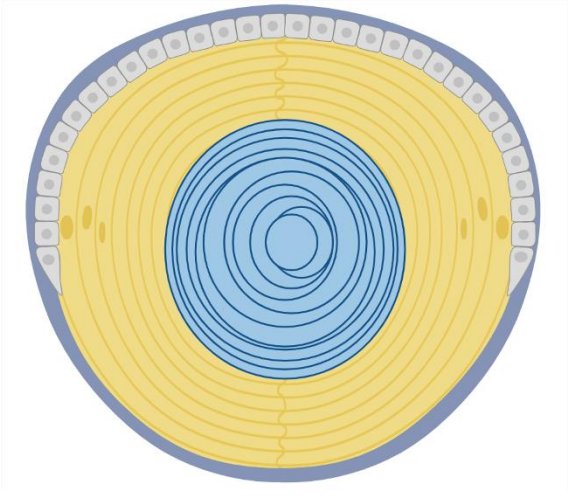

Figure 1. Diagram of the zebrafish lens. Epithelial cells (light gray) differentiate into lens fiber cells. The outer layer of lens fiber cells is the cortex (yellow), while the inner layer is the nucleus (blue). The lens is enclosed in the capsule, which is comprised of basement membrane (dark gray). Figure created using Biorender.com.

Abundance-based data-dependent acquisition (DDA) mass spectrometry proteomics and labeling methods such as tandem mass tags have been used to quantify proteins and post-translational modifications in the lens.[7–12] However, due to the high concentration of crystallins, up to 300 mg/mL in the human lens, these methods are challenged to identify and quantify low-abundance proteins.[13] Thus, new data-independent acquisition (DIA) mass spectrometry proteomics methods were developed to study the human lens proteome.[14,15] Using a 95-minute liquid chromatography gradient combined with a library-free DIA method on an Orbitrap Exploris 480 instrument to interrogate the human lens proteome, Cantrell and Schey identified 39,292 peptides, corresponding to 4,476 protein groups in the lens cortex. In contrast, a DDA method on the same

instrument identified 9,448 peptides and 1,739 corresponding protein groups in the lens cortex. These results show that by using DIA there was an almost 250% increase in peptide identifications and an almost 400% increase in protein group identifications. Fewer peptides and protein groups were identified in the lens nucleus region relative to the cortex, but the DIA method also identified more peptides and protein groups than the DDA method. diaPASEF (data independent acquisition parallel accumulation serial fragmentation) mass spectrometry proteomics, takes advantage of an additional ion mobility gas phase separation device and high-speed mass analysis to increase the number of peptide and protein group identifications.[16] Here, we pioneer the use of diaPASEF mass spectrometry proteomics to study the zebrafish lens and compare our results to data acquired using the previously reported orbitrap DIA method on the same tissue.

Previously, limited zebrafish lens proteomic analyses have been published, focusing either on development or quantifying changes in α-crystallin abundance using DDA mass spectrometry proteomics.[17–20] Zebrafish have several attributes that make them ideal model organisms for studying the lens proteome. For instance, zebrafish undergo a similar lens organogenesis process and have an analogous lens structure to humans.[21,22] However, the zebrafish lens has traditionally been analyzed intact due to its small size. Thus, for the first time, the nuclear and cortical regions of the zebrafish lens were separated for proteomic analysis, allowing for the examination of lens fiber cell aging. By utilizing diaPASEF proteomics, we collected the most comprehensive proteomic dataset of the zebrafish lens to date.

Materials and Methods

All reagents were purchased from Sigma-Aldrich (St. Louis, MO) and S-Trap micro columns were acquired from Protifi (Farmingdale, NY). Mass spectrometry grade trypsin and other remaining materials were purchased from Fisher Scientific (Waltham, MA) unless noted otherwise.

Zebrafish Maintenance and Breeding

AB-wild type strain zebrafish (Danio rerio) embryos were raised to 10 months of age. Zebrafish were kept in 30 mg/L instant ocean in deionized water at 28.5 °C and on a 14:10 hour light/dark cycle. The Vanderbilt University Institutional Animal Care and Use Committee authorized all zebrafish procedures.

Dissection and Separation of the Lens

Fresh lenses from three biological replicates were dissected from the eye and placed in cold PBS.[23] To separate the lens cortical and nuclear regions, 5 µL of cold 100 mM Tris pH 7.8, 1.5 mM ethylenediaminetetraacetic acid (EDTA) buffer was first placed in the neck of Biotik xPY4 20 µL pipette tips. Lenses were gently dried on a Kimwipe using tweezers and put into the buffer droplet in the pipette tip. The tips were spun at 5,000g for 30 seconds at 4 ºC in centrifuge tip adapters inserted into microcentrifuge tubes. The centrifugation process shears off the cortical region of the lens into the eluted solution while the lens nucleus remains intact and stuck in the tip. The tips were then cut using a razor blade at a point just below where the lens nucleus was held. Tweezers were used to free the nucleus by pushing it towards the larger end of the tips and spinning again to elute the intact nucleus into the buffer containing the separated cortex region. To wash the tips of any lingering cortical tissue, 10 µL of cold buffer was added and the tips were spun again. The buffer containing the cortical region was then transferred to another tube, leaving the intact nucleus inside the initial tube. The exterior of the nucleus was then washed by suspending it in 10 µL of cold buffer to remove any remaining attached cortical fiber cells. The wash buffer was then transferred to the cortical fraction and the separated regions were then snap-frozen for storage at -80 ºC.

Preparation of samples for mass spectrometry proteomic analysis

Separated tissue samples were thawed and 50 µL of 100 mM Tris pH 7.8, 1.5 mM EDTA, 5% sodium dodecyl sulfate (SDS) buffer was added to the nuclear samples, while 25 µL of 100 mM

Tris pH 7.8, 1.5 mM EDTA, 10% SDS buffer was added to the cortical samples. All samples were homogenized using an electric pestle and spun down at 18,213g for 5 minutes to pellet tissue. Protein concentration in the supernatant was measured using a bicinchoninic assay. Cysteines in 10 µg of protein were reduced for 1 hour at 56 °C using 10 mM of dithiothreitol and alkylated for 30 minutes in the dark at room temperature using 50 mM of iodoacetamide. Proteins were acidified by adding a 1:10 ratio of 27.5% phosphoric acid and then precipitated onto an S-Trap micro spin column by adding a 6:1 ratio of 100 mM triethylammonium bicarbonate (TEAB) in 90% methanol to sample and centrifuged at 4,000g for 30 seconds. Samples were washed three times with 50% chloroform/50% methanol, followed by four additional washes with 100 mM TEAB in 90% methanol. Proteins were digested by adding 50 mM TEAB with a 1:10 ratio of 10 µg sample to 1 µg of mass spectrometry grade trypsin and incubated for 2 hours at 47 °C. Digested peptides were eluted from S-trap sequentially by adding 50 mM TEAB, 0.2% formic acid (FA), 50% acetonitrile, and 0.2% FA solutions and centrifuging at 4,000g for 1 minute each. Eluted peptides were dried with a vacuum concentrator and stored at -80 ºC.

Data Acquisition

Peptides were resuspended in 0.2% FA to a concentration of 200 ng/µL. Peptide concentrations were estimated using a Nanodrop 2000 Spectrophotometer (Thermo Scientific), and samples were adjusted to 50 ng/µL. 0.015% n-dodecyl-ß-D-maltoside was added to diaPASEF samples. diaPASEF data were acquired on 150 ng of peptides using a 30-minute aqueous to organic gradient method delivered via a nanoELUTE2 on a PepSep column with 75-micron internal diameter, 25 cm length, and 1.5-micron particle size coupled to a timsTOF HT instrument (Bruker) using a 20-micron Captive Spray emitter. diaPASEF data were collected in 12 PASEF ramps from 0.75 to 1.3 $1/k_0$ covering 350 to 1250 m/z via variable windows ranging in size from 12.27-122.81 Th with 50 ms accumulation time. Orbitrap DIA data were acquired on 150 ng of peptides using a 95-minute aqueous to organic gradient method delivered via a Dionex Ultimate 3000 UHPLC on

a 360 µm outer diameter × 100 µm internal diameter column packed with 20 cm of 3 µm C18 reverse phase material (Jupiter, Phenomenex) coupled to an Orbitrap Exploris 480 instrument (Thermo Scientific). Precursor spectra from 385-1025 m/z were collected after thirty 20 m/z windows of DIA MS/MS spectra from 400-1000 m/z or thirty-one 20 m/z windows of DIA MS/MS spectra from 390-1010 m/z.[14,15]

Data Analysis and Visualization

Database searching for all files was performed using DIA-NN 1.9 with the default library-free settings and the reannotate and contaminants options selected.[24,25] A UniProt Swiss-Prot and TrEMBL zebrafish FASTA database (UP000000437, downloaded 9/10/2024, 25,999 entries with only one protein per gene) was used. Match between runs was turned on and MS1 and MS2 mass accuracy were fixed at 10 ppm. The default fixed N-terminal methionine excision and cysteine carbamidomethylation modifications and no variable modifications were selected. Searching was performed on an Intel Core i7-10700 CPU at 2.90 GHz.

Data were analyzed and visualized using custom R scripts on non-contaminant peptides having < 1% q-value and at least 2 unique peptides per protein group. DIA-NN normalization was rejected, and median normalization was performed separately on files for each instrument (Supplemental Figure 1).[14,15] Abundances were calculated using the diann_maxlfq function from the diann R package.[24] Figures were generated in R using ggplot2, ggvenn, and EnhancedVolcano packages. The prcomp package was used to perform principal component analysis (PCA) on un-transformed for all protein groups without missing values in the diaPASEF and orbitrap DIA datasets separately. A Welch's t-test between cortical and nuclear samples was performed on all proteins. Results were plotted using a volcano plot with significance cutoffs at 0.05 *p* value and +/- 1.5 $\log_2$ fold change. PANTHER was used for overrepresentation analyses of all proteins with a significant *p* value < 0.05 as determined via Welch's t-test using the 06/17/2024 GO database.[26] Statistically significant cortical and nuclear proteins from the

diaPASEF and orbitrap DIA datasets were analyzed separately using a Fisher's exact test with false discovery rate (FDR) calculated. All identified proteins from both data acquisitions comprised the reference proteome, and only parent GO terms with FDR *p* value < 0.05 were considered. Data are available via ProteomeXchange with identifier PXD059560.

Results and Discussion

Due to the additional gas phase separation and the higher instrument acquisition speed, the diaPASEF method was predicted to increase the number of peptide and corresponding protein group identifications relative to orbitrap DIA in the zebrafish lens cortex and nucleus. Results revealed that among three biological replicates an average of 3,584 unique peptides were identified using an orbitrap DIA method in the zebrafish cortex and an average of 3,103 unique peptides were identified in the zebrafish nucleus. However, by using diaPASEF these numbers increased to an average of 13,721 unique peptides identified in the zebrafish lens cortex and 11,996 unique peptides in the nucleus, representing about a 260% average increase in peptide identifications in both regions (Figure 2A). In the orbitrap DIA dataset, these peptides can be assigned, on average, to 511 unique protein groups in the cortex, and 432 unique protein groups in the nucleus. In the diaPASEF dataset, these numbers increased to an average of 1,537 unique

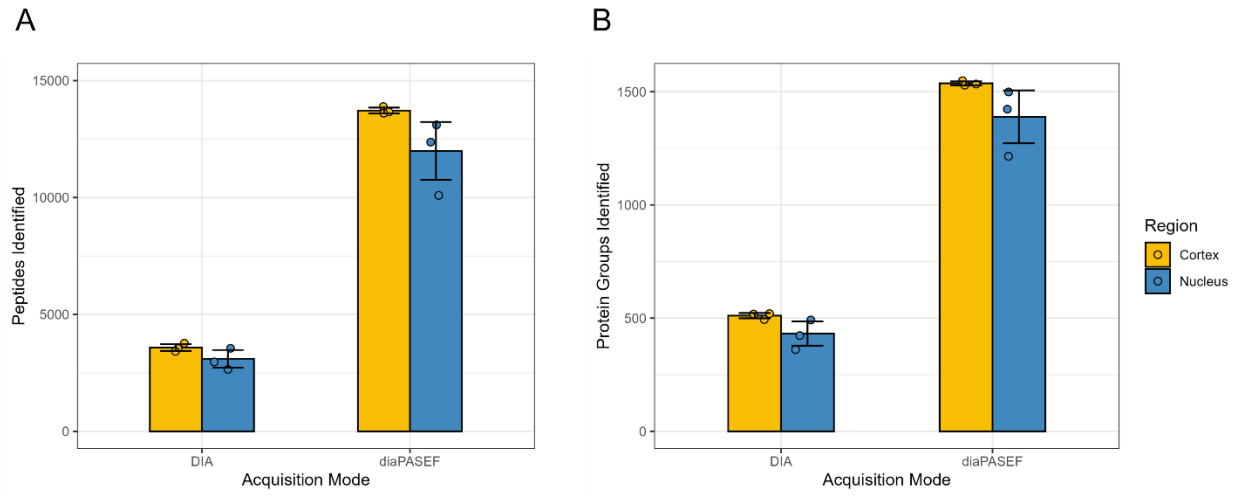

Figure 2. Bar plots of orbitrap DIA and diaPASEF results for three biological replicates displayed by acquisition mode and region. A) number of peptides identified and **B)** number of corresponding protein groups identified. A total of 16,718 unique peptides and 1,674 protein groups were identified throughout all sample types and data acquisition strategies.

protein groups in the cortex and an average of 1,389 unique protein groups in the nucleus (Figure 2B). These identifications represent about a 330% increase in cortical protein group identifications and about a 310% increase in nuclear protein group identifications using diaPASEF.

We next compared the overlap between identifications on the peptide and protein group level in the zebrafish cortex and nucleus for both data acquisition methods. On the peptide level, about 20% of all identifications in the lens cortex and nucleus were detected using both orbitrap DIA and diaPASEF. However, over 70% of all identified peptides were found exclusively in the diaPASEF datasets in both regions, suggesting ion mobility is needed to identify these additional peptides (Figure 3A) within a faster acquisition time. At the protein group level, there was more overlap, with more than 30% of all protein groups identified in both regions using both acquisition

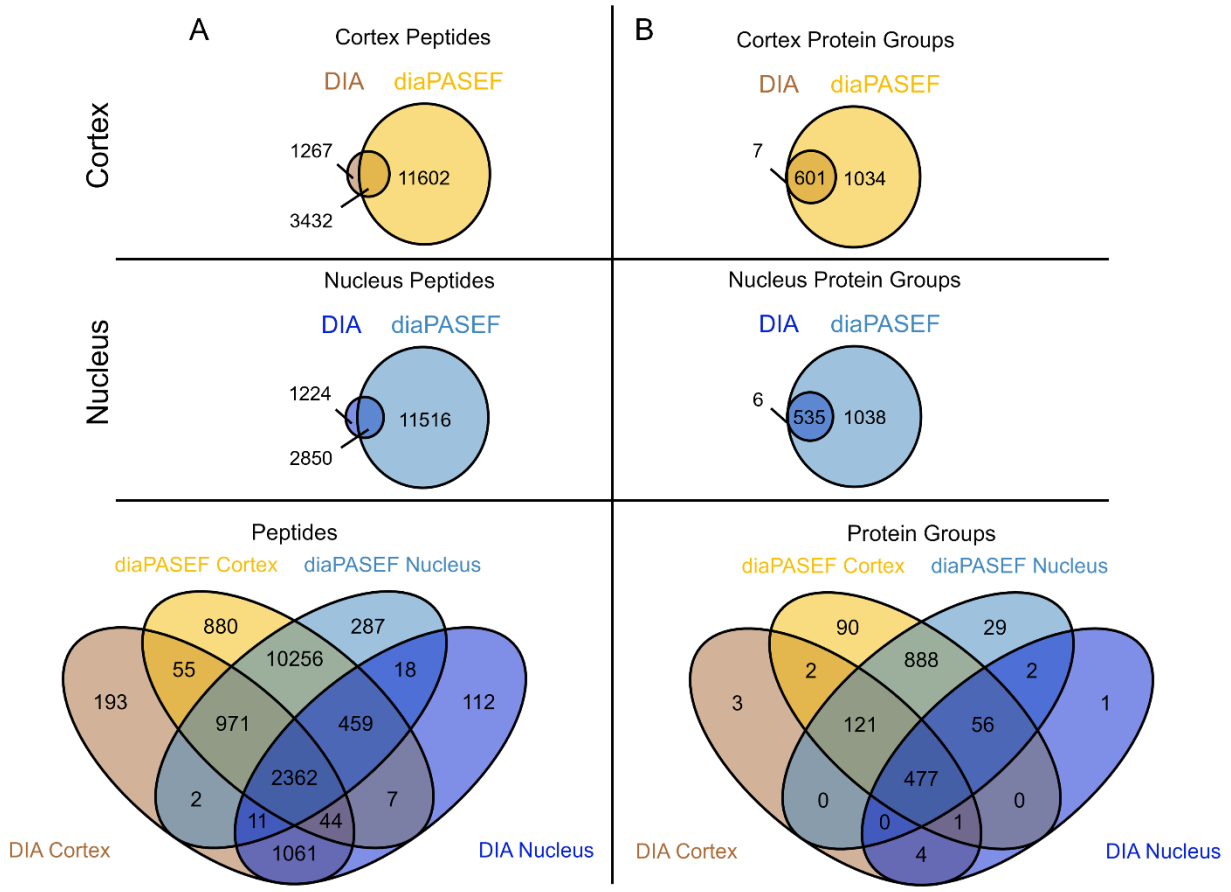

Figure 3. Venn diagrams showing the overlap between acquisition methods for A) peptides and **B)** corresponding protein groups identified in the zebrafish lens cortex and nucleus. All peptides and protein groups found in at least one biological replicate were considered, with duplicates removed.

methods. Over 60% of all protein groups were found only in the diaPASEF datasets for both regions, suggesting that diaPASEF gives a more complete protein coverage in the zebrafish lens (Figure 3B). The diaPASEF datasets also had, compared to the orbitrap DIA datasets, a lower median MS2-based peptide intensity percent coefficient of variation (% CV) and proportion of peptides with a lower % CV (Supplemental Figure 2A and 2B).

Additionally, there is a notable overlap between the cortex and nucleus regions in identifications on both the peptide and protein group levels in both data acquisition methods (Supplemental Figure 3A and 3B). Differences in peptide and protein group identifications were likely due to protein modification, truncation, degradation, or differences in protein synthesis pathways, processes associated with nuclear fiber cell protein aging.[5,11,27,28] A high degree of similarity was also found between replicates (Supplemental Figure 4). However, unique peptides and protein groups found in only one replicate are likely a result of low abundance peptides being less reproducible and the high biological variance found in zebrafish.[29–31] These results demonstrate that diaPASEF facilitates the quantification of more unique peptides and protein groups in the zebrafish lens compared to the orbitrap DIA method, allowing for deeper investigation into lens biology.

Next, we validated the separation of the zebrafish lens cortex and nucleus regions observed proteins in the diaPASEF dataset. A PCA plot using untransformed MaxLFQ quantities for 1,103 protein groups found in all diaPASEF samples showed that the samples were separated into two distinct clusters: cortical and nuclear (Figure 4A). The same pattern was observed in the orbitrap DIA data (Supplemental Figure 5A).

Additionally, protein abundances were compared between the nuclear and cortical diaPASEF datasets via a volcano plot to identify differentially expressed proteins. No imputation was performed and only proteins found in all three replicates were considered (Figure 4B). The results revealed that several ribosomal proteins such as Rps8, Rpl8, Rpl13, and Zgc:171772 were differentially expressed in the cortex relative to the nucleus. The differential expression of

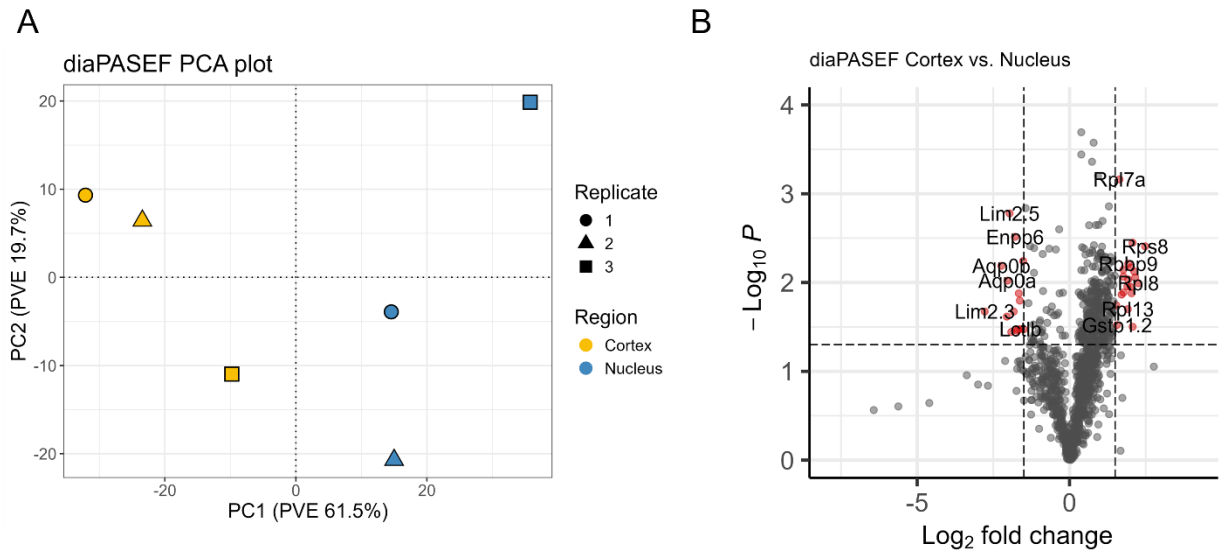

Figure 4. Analysis of diaPASEF data. A) PCA plot separated by replicate and region (n = 1,103). **B)** Volcano plot of cortex vs nucleus sample proteins. Significant protein groups are shown in red with cut-offs of $\log_2$FC > 1.5 or $\log_2$FC < -1.5 and p value < 0.05 as calculated from Welch's t-test.

ribosomal proteins is consistent with known biology in that protein translation occurs in cortical fiber cells and that organelles are degraded during fiber cell differentiation, leading to a loss of ribosomal proteins in fully differentiated nuclear fiber cells.[1] Our results also show that Gstp1.2, an enzyme involved in the conjugation of glutathione, is differentially expressed in the cortex. Glutathione is a major lens antioxidant important in preventing cataract formation.[32,33]

In the lens nucleus, structural membrane proteins, such as Lim 2.5, Aqp0a, and Aqp0b were differentially expressed.[34] In particular, Aqp0a, Aqp0b, Gja8b, and Slc20a1b are all part of the lens microcirculation system that imports nutrients and exports waste products to and from the lens nucleus.[35–38] Metabolically active proteins, such as Enpp6 and Lctlb were also differentially expressed in the lens nucleus, suggesting that some metabolically active proteins are retained after lens fiber cell differentiation. Lctlb has also been shown to be involved in lens suture and cataract formation in mice.[39,40] These results showed that overall, more lens-specific proteins expressed during lens fiber cell differentiation were found in the nuclear region, indicative of the successful separation of the lens cortex and nucleus. A full list of significant proteins, as visualized in the volcano plot, is provided in Supplemental Table 1. Similar trends were also

observed in the orbitrap DIA method volcano plot (Supplemental Figure 5B). Significant proteins in the orbitrap DIA method volcano plot are shown in Supplemental Table 2. Only 5 significant proteins were found in both datasets, Rpl13, Gstp1.2, Si:dkey-164f24.2, Lctlb, and Aqp0b. Of the 24 remaining non-overlapping significant proteins identified in the DIA dataset, 23 were not significant in the diaPASEF dataset, and 1 was detected exclusively in the DIA dataset. However, 22 out of these 23 proteins met the *p* value cut-off but did not meet the log_2FC cut-off. Therefore, in the diaPASEF dataset there was a statistically significant but small difference between the expression of these proteins in the cortex and the nucleus. This can be due to differences such as duty cycle, dynamic range, and sensitivity between the instruments and methods.

Table 1. Overrepresentation analysis of statistically significant cortical diaPASEF proteins (*p* value < 0.05 and log_2FC > 1.5).

GO Term	Annotation	# in Set	Fold Enrichment	FDR
GO Biological Process				
GO:0006412	Translation	15	7.94	8.55E-09
GO Molecular Function				
GO:0003735	Structural constituent of ribosome	15	16.4	0.344
GO Cellular Component				
GO:0022625	Cytosolic large ribosomal subunit	12	24.32	1.54E-13

Finally, we performed an overrepresentation analysis for significant proteins identified via Welch's t-test for both diaPASEF cortical and nuclear datasets using PANTHER.[26] In the cortex diaPASEF dataset, there is an overrepresentation of ribosomal and translation-associated gene ontologies (Table 1).

Table 2. Overrepresentation analysis of statistically significant nuclear diaPASEF proteins (*p* value < 0.05 and log_2FC < -1.5).

GO Term	Annotation	# in Set	Fold Enrichment	FDR
GO Biological Process				
No statistically significant results				
GO Molecular Function				
GO:0005372	Water transmembrane transporter activity	2	> 100	5.20E-02
GO:0004096	Catalase activity	2	> 100	3.46E-02
GO Cellular Component				
GO:0005911	Cell-cell junction	4	11.36	2.31E-02
GO:0005886	Plasma membrane	10	4.33	2.95E-03
GO:0005737	Cytoplasm	3	0.28	8.07E-03

Conversely, the diaPASEF nucleus dataset exhibits an overrepresentation of water

transmembrane transporter activity, catalase activity, cell-junction, cytoplasmic, and membrane gene ontologies (Table 2). These gene ontology results further validate the successful separation of the younger organelle-containing lens cortex from the older organelle-free lens nucleus. Overrepresentation analysis results for the orbitrap DIA cortex dataset are shown in Supplemental Table 3. No overrepresentation analysis was performed on the orbitrap DIA nucleus dataset, due to the low number of significantly expressed proteins.

Conclusion

We have shown that a 30-minute liquid chromatography diaPASEF method on a timsTOF instrument identifies more peptide and protein groups in the lens than a 95-minute liquid chromatography DIA method on an orbitrap instrument due to a faster acquisition time and the addition of ion mobility. Thus, using diaPASEF, we have collected the most comprehensive zebrafish lens proteome dataset to date. Through the analysis of the diaPASEF dataset, we have also demonstrated the first instance of successful separation of the zebrafish lens cortex and nucleus regions. diaPASEF is a methodology that will allow further probing of the lens proteome using model organisms to more thoroughly understand lens biology.

Supporting Information

Median normalization boxplots, peptide intensity percent CV per sample, venn diagrams comparing overlap between regions, venn diagrams comparing overlap between replicates, orbitrap DIA PCA and volcano plots, tables of significant proteins identified in diaPASEF and orbitrap DIA datasets, significant GO terms for orbitrap DIA cortex dataset (PDF)

Acknowledgments

We thank Zhen Wang, Lee Cantrell, and the Mchaourab lab for critical discussions about this manuscript. The authors would also like to acknowledge support from the Vanderbilt Mass

Spectrometry Research Center and NIH grants T32 GM065086 (SRZ), T32 EY007135 (SRZ), R01 EY012018 (HSM), P30 EY008126 (KLS), and R01 EY024258 (KLS).

References

1. Bassnett, S. On the mechanism of organelle degradation in the vertebrate lens. *Exp. Eye Res.* **88**, 133 (2009).
2. Kuszak, J. R., Zoltoski, R. K. & Sivertson, C. Fibre cell organization in crystalline lenses. *Exp. Eye Res.* **78**, 673–687 (2004).
3. Greiling, T. M. S., Aose, M. & Clark, J. I. Cell fate and differentiation of the developing ocular lens. *Invest. Ophthalmol. Vis. Sci.* **51**, 1540–1546 (2010).
4. Vorontsova, I., Hall, J. E. & Schilling, T. F. Assessment of Zebrafish Lens Nucleus Localization and Sutural Integrity. *J. Vis. Exp. JoVE* (2019) doi:10.3791/59528.
5. Schey, K. L., Wang, Z., Friedrich, M. G., Garland, D. L. & Truscott, R. J. Spatiotemporal Changes in the Human Lens Proteome: Critical Insights into Long-lived Proteins. *Prog. Retin. Eye Res.* **76**, 100802 (2019).
6. Wang, Z. & Schey, K. L. Quantification of thioether-linked glutathione modifications in human lens proteins. *Exp. Eye Res.* **175**, 83 (2018).
7. Hains, P. G. & Truscott, R. J. W. Proteomic analysis of the oxidation of cysteine residues in human age-related nuclear cataract lenses. *Biochim. Biophys. Acta* **1784**, 1959–1964 (2008).
8. Whitson, J. A. *et al.* Proteomic analysis of the glutathione-deficient LEGSKO mouse lens reveals activation of EMT signaling, loss of lens specific markers, and changes in stress response proteins. *Free Radic. Biol. Med.* **113**, 84–96 (2017).
9. Khan, S. Y. *et al.* Proteome Profiling of Developing Murine Lens Through Mass Spectrometry. *Invest. Ophthalmol. Vis. Sci.* **59**, 100–107 (2018).

10. Giblin, F. J. *et al*. Acceleration of age-induced proteolysis in the guinea pig lens nucleus by in vivo exposure to hyperbaric oxygen: A mass spectrometry analysis. *Exp. Eye Res.* **210**, 108697 (2021).
11. Wang, Z., Han, J., David, L. L. & Schey, K. L. Proteomics and Phosphoproteomics Analysis of Human Lens Fiber Cell Membranes. *Invest. Ophthalmol. Vis. Sci.* **54**, 1135 (2013).
12. Zhou, H. Y. *et al*. Quantitative proteomics analysis by iTRAQ in human nuclear cataracts of different ages and normal lens nuclei. *Proteomics Clin. Appl.* **9**, 776–786 (2015).
13. Gillet, L. C. *et al*. Targeted Data Extraction of the MS/MS Spectra Generated by Data-independent Acquisition: A New Concept for Consistent and Accurate Proteome Analysis. *Mol. Cell. Proteomics MCP* **11**, O111.016717 (2012).
14. Cantrell, L. S. & Schey, K. L. Data-Independent Acquisition Mass Spectrometry of the Human Lens Enhances Spatiotemporal Measurement of Fiber Cell Aging. *J. Am. Soc. Mass Spectrom.* **32**, 2755–2765 (2021).
15. Cantrell, L. S., Gletten, R. B. & Schey, K. L. Proteome Remodeling of the Eye Lens at 50 Years Identified With Data-Independent Acquisition. *Mol. Cell. Proteomics MCP* **22**, (2023).
16. Meier, F. *et al*. diaPASEF: parallel accumulation–serial fragmentation combined with data-independent acquisition. *Nat. Methods* **17**, 1229–1236 (2020).
17. Posner, M. *et al*. The zebrafish as a model system for analyzing mammalian and native α-crystallin promoter function. *PeerJ* **5**, e4093 (2017).
18. Wages, P., Horwitz, J., Ding, L., Corbin, R. W. & Posner, M. Changes in zebrafish (Danio rerio) lens crystallin content during development. *Mol. Vis.* **19**, 408 (2013).
19. Greiling, T. M. S., Houck, S. A. & Clark, J. I. The zebrafish lens proteome during development and aging. *Mol. Vis.* **15**, 2313 (2009).

20. Posner, M. *et al.* A proteome map of the zebrafish (Danio rerio) lens reveals similarities between zebrafish and mammalian crystallin expression. *Mol. Vis.* **14**, 806–814 (2008).
21. Liu, C. F. *et al.* Zebrafish (Danio rerio) Is an Economical and Efficient Animal Model for Screening Potential Anti-cataract Compounds. *Transl. Vis. Sci. Technol.* **11**, (2022).
22. Hong, Y. & Luo, Y. Zebrafish Model in Ophthalmology to Study Disease Mechanism and Drug Discovery. *Pharm. Basel Switz.* **14**, (2021).
23. Park, J., MacGavin, S., Niederbrach, L. & Mchaourab, H. S. Interplay between Nrf2 and αB-crystallin in the lens and heart of zebrafish under proteostatic stress. *Front. Mol. Biosci.* **10**, 1185704 (2023).
24. Demichev, V., Messner, C. B., Vernardis, S. I., Lilley, K. S. & Ralser, M. DIA-NN: neural networks and interference correction enable deep proteome coverage in high throughput. *Nat. Methods 2019 171* **17**, 41–44 (2019).
25. Demichev, V. *et al.* dia-PASEF data analysis using FragPipe and DIA-NN for deep proteomics of low sample amounts. *Nat. Commun.* **13**, 3944 (2022).
26. Thomas, P. D. *et al.* PANTHER: a library of protein families and subfamilies indexed by function. *Genome Res.* **13**, 2129–2141 (2003).
27. MacCoss, M. J. *et al.* Shotgun identification of protein modifications from protein complexes and lens tissue. *Proc. Natl. Acad. Sci. U. S. A.* **99**, 7900–7905 (2002).
28. Cantrell, L. S. & Schey, K. L. Proteomic Characterization of the Human Lens and Cataractogenesis. *Expert Rev. Proteomics* **18**, 119–135 (2021).
29. Brown, K. H. *et al.* Extensive genetic diversity and substructuring among zebrafish strains revealed through copy number variant analysis. *Proc. Natl. Acad. Sci.* **109**, 529–534 (2012).
30. Guryev, V. *et al.* Genetic variation in the zebrafish. *Genome Res.* **16**, 491–497 (2006).

31. Parichy, D. M. Advancing biology through a deeper understanding of zebrafish ecology and evolution. *eLife* **4**, e05635 (2015).

32. Giblin, F. J. Glutathione: a vital lens antioxidant. *J. Ocul. Pharmacol. Ther. Off. J. Assoc. Ocul. Pharmacol. Ther.* **16**, 121–135 (2000).

33. Reddy, V. & Giblin, F. J. Metabolism and function of glutathione in the lens. *Ciba Found. Symp.* **106**, 65–87 (1984).

34. Maher, G. J., Black, G. C. & Manson, F. D. Focus on Molecules: Lens intrinsic membrane protein (LIM2/MP20). *Exp. Eye Res.* **103**, 115–116 (2012).

35. Vaghefi, E. & Donaldson, P. J. The lens internal microcirculation system delivers solutes to the lens core faster than would be predicted by passive diffusion. *Am. J. Physiol. - Regul. Integr. Comp. Physiol.* **315**, R994–R1002 (2018).

36. Donaldson, P. J., Musil, L. S. & Mathias, R. T. Point: A Critical Appraisal of the Lens Circulation Model—An Experimental Paradigm for Understanding the Maintenance of Lens Transparency? *Invest. Ophthalmol. Vis. Sci.* **51**, 2303–2306 (2010).

37. Schey, K. L., Petrova, R. S., Gletten, R. B. & Donaldson, P. J. The Role of Aquaporins in Ocular Lens Homeostasis. *Int. J. Mol. Sci.* **18**, 2693 (2017).

38. Mathias, R. T., White, T. W. & Gong, X. Lens Gap Junctions in Growth, Differentiation, and Homeostasis. *Physiol. Rev.* **90**, 179 (2010).

39. Wang, Z., Cantrell, L. S. & Schey, K. L. Spatially Resolved Proteomic Analysis of the Lens Extracellular Diffusion Barrier. *Invest. Ophthalmol. Vis. Sci.* **62**, 25 (2021).

40. Fan, J. *et al.* The klotho-related protein KLPH (lctl) has preferred expression in lens and is essential for expression of clic5 and normal lens suture formation. *Exp. Eye Res.* **169**, 111–121 (2018).